PROFESSOR BALAKUNTALAM KASINATH (Orcid ID : 0000-0002-6360-101X)

Article type : Original Paper

Chloride channel accessory 1 integrates chloride channel activity and mTORC1 in aging related kidney injury

Hak Joo Lee, PhD[1], Andrew Donati, MD[1], Denis Feliers, PhD[1,*], Yuyang Sun, PhD[2], Yanli Ding, MD[3] , Muniswamy Madesh, PhD[1], Adam B. Salmon, PhD[4,5,6,7], Yuji Ikeno, MD, PhD[3,4,6], Corinna Ross, PhD[8,9], Christopher L. O'Connor[10], Wenjun Ju, PhD[10], Markus Bitzer, MD[10], Yidong Chen, PhD[11, 12], Goutam Ghosh Choudhury, PhD[1,6,7], Brij B. Singh, PhD[2], Kumar Sharma, MD[1,6], and, Balakuntalam S. Kasinath, MD[1,5,6,7]

[1]Center for Renal Precision Medicine, Department of Medicine, University of Texas Health, San Antonio, TX

[2]Department of Periodontics, University of Texas Health, San Antonio, TX

[3]Department of Pathology, University of Texas Health, San Antonio, TX

[4]Department of Molecular Medicine, University of Texas Health, San Antonio, TX

[5]Barshop Institute for Longevity and Aging Studies, University of Texas Health, San Antonio, TX,

[6]South Texas Veterans Health Care System, San Antonio, TX

[7]Geriatric Research, Education & Clinical Center, South Texas Veterans Health Care System, San Antonio, TX

[8]Southwest National Primate Research Center, Texas Biomedical Research Institute, San Antonio, TX,

[9]Department of Science and Mathematics, Texas A&M University San Antonio, San Antonio, TX

[10]Department of Internal Medicine, University of Michigan, Ann Arbor, MI,
[11]Department of Population Health Sciences, University of Texas Health, San Antonio, TX
[12]Greehey Children's Cancer Research Institute, University of Texas Health, San Antonio, TX

*DF is now with Genomic Institute of the Novartis Research Foundation, La Jolla, CA.

Running title: CLCA1 in aging related kidney injury

Correspondence: B. S. Kasinath, MD
Division of Nephrology, Department of Medicine, MC7882
University of Texas Health at San Antonio
7703 Floyd Curl Drive
San Antonio, TX 78229
Email: kasinath@uthscsa.edu
Phone 210-326-0929

Checklist

Total Character Count:	43,031
Word count of the Summary:	250
Number of papers cited in the References:	58
A listing of all Tables:	Supplementary Tables: 2

A listing of all Figures:

Fig. 1	Color	2-column format
Fig. 2	Color	2-column format
Fig. 3	Color	2-column format
Fig. 4	Black and White	2-column format
Fig. 5	Black and White	2-column format
Fig. 6	Color	2-column format

Supplementary Figures: S1-S2

Summary

The mechanisms of kidney injury in aging are not well understood. In order to identify hitherto unknown pathways of aging related kidney injury we performed RNA-Seq on kidney extracts of young and aged mice. Expression of Chloride (Cl) channel accessory 1 (*Clca1)* mRNA and protein was increased in the kidneys of aged mice. Immunostaining showed a marked increase in CLCLA1 expression in the proximal tubules of the kidney from aged mice. Increased kidney *CLCA1* gene expression also correlated with aging in marmosets and in a human cohort. In aging mice, increased renal cortical CLCA1 content was associated with hydrogen sulfide (H_2S) deficiency, which was ameliorated by administering sodium hydrosulfide (NaHS), a source of H_2S. In order to study whether increased CLCA1 expression leads to injury phenotype and the mechanisms involved, stable transfection of proximal tubule epithelial cells overexpressing human CLCA1 (hCLCA1) was performed. Overexpression of hCLCA1 augmented Cl^- current via the Ca^{++}-dependent Cl^- channel TMEM16A (anoctamin-1) by patch clamp studies. hCLCA1 overexpression also increased the expression of fibronectin, a matrix protein, and induced the senescence-associated secretory phenotype (SASP). Mechanistic studies underlying these changes showed that hCLCA1 overexpression leads to inhibition of AMPK activity and stimulation of mTORC1 as cellular signaling determinants of injury. Both TMEM16A inhibitor and NaHS reversed these signaling events and prevented changes in fibronectin and SASP. We conclude that CLCA1-TMEM16A-Cl^- current pathway is a novel mediator of kidney injury in aging that is regulated by endogenous H_2S.

Key words: Ion transport, Fibrosis, Senescence associated secretory phenotype

Introduction

Accumulation of matrix proteins leading to glomerular and tubulo-interstitial fibrosis is a major contributor to kidney injury in aging. Unabated tubulo-interstitial fibrosis of the kidney is a major determinant of progressive loss of kidney function (Humphreys 2018). These structural changes and proteinuria are evident in aging mice and aging nonhuman primates (marmosets) (Zheng et al., 2003; Wu et al., 2010; Sataranatarajan et al., 2012; Bitzer & Wiggins 2016; Lee et al., 2018; Lee et al., 2019). Current therapeutic approaches to inhibit kidney fibrosis are limited; while they may slow the progressive loss of kidney function, they are not able to halt it altogether. Thus, there is an urgent need to identify novel mechanisms so that interventions may be developed to arrest chronic kidney injury and functional loss encountered in aging.

Accordingly, we took a discovery approach to identify novel mRNA transcripts that may be involved in kidney aging. RNA-Seq revealed increase in the expression of *Clca1* mRNA in the aged kidney. CLCA1 facilitates Cl^- current operated by TMEM16A (anoctamin-1), a Ca^{++}-dependent Cl^- channel (Verkman & Galietta 2009; Jentsch & Pusch 2018). Cl^- movement accompanied by cations such as Na^+ and K^+ or in exchange for other anions occurs among fluid compartments in many segments of the kidney tubule. Cl^- shift among these compartments is governed by electrochemical potential and transporters and exchangers.

CLCA1 functions as a self-cleaving protease forming C-terminal and N-terminal fragments (Sala-Rabanal et al., 2015). The N-terminal fragment (~72 kDa) associates with the extracellular domain of TMEM16A to stimulate Cl^- movement in a Ca^{++}-dependent manner (Sala-Rabanal et al., 2017). CLCA1 promotes cell membrane retention of TMEM16A rather than increase its expression (Sala-Rabanal et al., 2015). The role played by this system has not been explored in aging related changes in the kidney. For the first time, we explored the role of CLCA1 in kidney injury in aging.

Results

CLCA1 expression is increased in the aged kidney: RNA-Seq performed on renal cortex of male young and aged mice showed that more than 400 mRNAs

underwent a significant change with age (Fig. 1A, B, Suppl. Table 1). Top hits and their possible functional import are shown in in Suppl. Table 2. *Clca1* was among mRNAs that showed a robust increase with age (adjusted $P = 4.92 \times 10^{-16}$). We confirmed changes in *Clca1* found by RNA-Seq by directly analyzing mRNA and protein levels in samples from aged kidneys; we confirmed that *Clca1* mRNA and the corresponding protein levels were increased in the kidney cortex of aged mice (Fig. 1C, D). Aging was not associated with changes in the renal cortical expression of TMEM16A, a Ca^{++}-dependent Cl^- channel, the functional partner of CLCA1 (Fig. 1E). Gene Ontology (GO) analysis of cellular component of regulated renal cortical mRNAs in aged mice showed extracellular region part (Fisher's exact test, *P*-value = 3.50×10^{-12}) and extracellular space (Fisher's exact test, *P*-value = 6.0×10^{-9}) as major hits; these sites may correspond to Cl^- secretion that could involve CLCA1 (Fig. 1F). GO analysis for molecular function revealed anion transmembrane transporter activity (Fisher's exact test, $P = 6.40 \times 10^{-6}$), and secondary active transmembrane transporter activity (Fisher's exact test, $P = 1.50 \times 10^{-8}$) among the top hits (Fig. 1G); these functions also could correspond to CLCA1 as a facilitator of Cl^- channel activity of TMEM16A, a transmembrane protein. GO analysis of biologic process identified small molecule metabolic process as one of the top hits (Fisher's exact test, $P = 1.70 \times 10^{-18}$, Fig. 1H), which could conceivably involve Cl^- transport. Thus, there was a congruence between changes in CLCA1 expression in the renal cortex of aged mice, and, spatial distribution and functional processes predicted by the GO analysis.

Immunohistochemistry showed a faint tubular expression of CLCA1 in the renal cortex of young mice; in aged mice, CLCA1 expression was robustly increased in the tubules including in the proximal tubules; there was some increase in the glomerular mesangium staining for CLCA1 also (Fig. 2A). H_2S is constitutively synthesized in the kidney and plays a highly nuanced role in kidney physiology and pathology (Kasinath et al., 2018). In the aging kidney, deficiency in the synthesis of H_2S is associated with accumulation of matrix proteins which contributes to renal fibrosis, inhibition of AMP-activated protein kinase (AMPK)

activity, and activation of mTORC1 (Sataranatarajan et al., 2012; Lee et al., 2018). Stimulation of mTORC1 is a major determinant of synthesis of proteins including matrix proteins (Sataranatarajan et al., 2007; Kasinath et al., 2009). Administration of H_2S in the form of NaHS to 18-19-month old mice for 5 months inhibits these signaling events and increase in matrix proteins, renal fibrosis, while also reducing albuminuria (Lee et al., 2018). These data showed a fundamental role for H_2S in aging associated kidney injury. We examined whether H_2S regulated kidney CLCA1 expression in aged mice. NaHS reduced the renal cortical expression of CLCA1 in aging mice compared to untreated aging mice (Fig. 2B, C).

To determine the potential evolutionary and clinical relevance of these findings, we also assessed the changes with age in CLCA1 expression in both non-human primate and human kidney samples. Aging is associated with robust kidney fibrosis in the marmoset (*Callithrix jacchus*), a nonhuman primate (Lee et al., 2019). On immunoblotting lysates from the kidney cortex of aged female marmosets, we found a significant increase in the expression of a 72 kDa fragment of CLCA1, which probably corresponds to its functional N-terminal domain that binds to TMEM16A to augment Cl^- current (Suppl. Fig. S1); a trend towards increase in the expression of the whole 130 kDa molecule was seen in the same animals ($p=0.08$). Changes in kidney cortical CLCA1 expression in the aged male marmosets did not reach clinical significance. We examined if similar changes were seen in kidneys from humans. There was a significant direct correlation between age and *CLCA1* expression in the kidney tubule interstitial compartment in a human cohort (Fig. 2D); this aligned with the increased tubular expression seen in aged mice (Fig. 2A). These data show the following: (1) Changes in renal cortical CLCA1 expression parallel kidney injury and its amelioration by NaHS in aging mice. (2) Tubular epithelial cells including those in the proximal tubules contribute to increase in kidney CLCA1 expression in aging. (3) Aging related increase in kidney CLCA1 expression is evolutionarily conserved.

CLCA1 overexpression induces mTORC1 and augments matrix protein content. We investigated if CLCA1-TMEM16A- Cl^- current system has a mechanistic role in kidney injury encountered in aging. Kidney matrix protein increase in aging mice is associated with mTORC1 activation (Lee et al., 2018). Whether CLCA1 has a role in this process is not known. We stably overexpressed FLAG-tagged human CLCA1 (hCLCA1) in a mouse proximal tubular epithelial cell line (MCT). This resulted in increased expression of both the full length ~130 kDa CLCA1 molecule and a ~72 kDa fragment, probably the N-terminal fragment, which associates with TMEM16A to promote Cl^- current Fig. 3A). However, TMEM16A expression was unchanged in hCLCA1 overexpressing cells (Fig. 3B). On whole cell patch clamp, Cl^- current was higher in hCLCA1 overexpressing cells indicating that the Cl^- channel activity of TMEM16A was increased; Cl^- current was completely inhibited by T16Ainh-A01, a selective TMEM16A inhibitor (Fig. 3C). Overexpression of hCLCA1 resulted in increase in fibronectin, a kidney matrix protein that is increased in the aging kidney (Lee et al., 2018; Lee et al., 2019) (Fig. 3D).

We explored signaling pathways that regulate synthesis of proteins including matrix proteins in the kidney. AMPK is an energy sensor that constitutively inhibits mTORC1 in controlling protein synthesis in the kidney (Lee et al., 2007; Kasinath et al., 2009). hCLCA1 overexpression inhibited AMPK activity as shown by reduction in the phosphorylation of acetyl CoA carboxylase (ACC), its direct substrate (Fig. 3E); increased phosphorylation of p70S6 kinase indicated mTORC1 activation (Fig. 3F). Rapamycin abolished the increase in fibronectin in hCLCA1 overexpressing cells (Fig. 3G) while inhibiting mTORC1 (Suppl. Fig. S2). Akt is upstream of mTORC1 in signaling pathways regulating protein synthesis (Kasinath et al., 2009). Akt phosphorylation of Ser473 was increased (Fig. 3H) suggesting mTORC2 activation (Sarbassov et al., 2005). Akt inhibits AMPK and increases activity of mTORC1 leading to stimulation of synthesis of proteins (Kasinath et al., 2009; Hawley et al., 2014). The reason for Akt phosphorylation by overexpression of CLCA1 is not clear; it is possible that it is linked to increasing Cl^- current at the cell surface. Changes in the

phosphorylation of AMPK, mTORC1, and Akt are identical to the data reported in the renal cortex of aging mice and marmosets.(Lee et al., 2018; Lee et al., 2019). These results show the following: (1) Overexpression of CLCA1 increases Cl^- current in proximal tubular epithelial cells. (2) It also activates Akt, inhibits AMPK, and stimulates mTORC1 leading to increased fibronectin expression.

CLCA1 overexpression promotes SASP. A subset of kidney cells including proximal tubular epithelial cells manifest SASP in aging mice, and interventions that reduce SASP ameliorate aging associated kidney injury (Baker et al., 2016; Lee et al., 2018). SASP has been linked to mTOR activation (Herranz et al., 2015). SASP involves secretion of pro-fibrotic factors that promote kidney fibrosis (Xu et al., 2020). Wnt9 - TGFβ1 pathway has been shown to be involved in this process (Luo et al., 2018). hCLCA1 overexpressing cells showed increased expression of p53, p21 and $p16^{INK4a}$, features of cell senescence (Fig. 4A-C). Cells manifesting SASP assume a pro-inflammatory phenotype; kidney content of IL-1β and IL-6 is increased in aging mice (Lee et al., 2018) Overexpression of hCLCA1 augmented the expression of IL-1α, IL-1β, and IL-6 (Fig. 4D-F) in agreement with the *in vivo* observations. Data in Figs. 3 and 4 show that hCLCA1 overexpression reproduces key aging associated changes in kidney matrix proteins, signaling pathways, and, SASP. These data implicate CLCA1 system in bringing about these aging-associated features in the kidney.

TMEM16A activity is required for CLCA1-induced changes. CLCA1 acts to facilitate Cl^- current generated by TMEM16A. Alternatively, it could have TMEM16A-independent actions. We explored whether the effects of CLCA1 overexpression required the activity of TMEM16A by employing T16Ainh-A01, a TMEM16A selective inhibitor that blocks the activity of the latter (Fig. 3C). The inhibitor abolished the increase in fibronectin induced by hCLCA1 overexpression without affecting the expression of hCLCA1 or TMEM16A (Fig. 5A-C). T16Ainh-A01 also inhibited features of SASP induced by hCLCA1 overexpression (Fig. 5D-H). These data demonstrate that the ability of CLCA1 to stimulate matrix protein synthesis and induce SASP in renal epithelial cells requires the activation of TMEM16A, the Ca^{++}-dependent Cl^- channel.

Effect of H_2S on CLCA1-induced changes: Recent findings indicate that gaseous molecules including H_2S are important regulators of kidney function (Feliers et al., 2016; Kasinath et al., 2018). H_2S is constitutively synthesized by the kidney (Lee et al., 2018; Lee et al., 2019). Proximal tubule epithelial cells and podocytes synthesize H_2S *in vitro* (Lee et al., 2012; Lee et al., 2017). Cystathionine γ-lyase (CSE) and cystathionine β-synthase (CBS) are involved in H_2S generation in the trans-sulfuration pathway (Kasinath et al., 2018). Kidney injury manifesting as matrix accumulation in diabetes is associated with decreased synthesis of H_2S (Lee et al., 2012); administration of H_2S ameliorates kidney injury in diabetic rodents (Zhou et al., 2014). We have reported that kidney H_2S generation is decreased in aging mice, and that administration of NaHS ameliorates matrix protein increase and SASP in them (Lee et al., 2018). We tested if there was an interaction between CLCA1 and H_2S. Overexpression of hCLCA1 reduced the expression of CSE but not of CBS; however, H_2S generation was unaffected (Fig. 6A, B) suggesting that CLCA1-independent mechanisms cause H_2S deficiency in the aging kidney. Interestingly, NaHS inhibited increase in fibronectin induced by hCLCA1 overexpression (Fig. 6C). We examined the signaling mechanism underlying NaHS effects. NaHS countered changes in the activity of AMPK and mTORC1 seen with overexpression of hCLCA1. Thus, NaHS restored AMPK activity and inhibited mTORC1 activity in hCLCA1 overexpressing cells (Fig. 6D, E). Additionally, NaHS abolished some aspects of SASP in hCLCA1 overexpressing cells (Fig. 6F, G). These effects of H_2S are in agreement with the data in aging mice that received NaHS (Lee et al., 2018). Overexpression of hCLCA1 resulted in increase in Cl^- current (Fig. 3C). Patch clamp studies showed that hCLCA1-induced Cl^- current was inhibited by NaHS (Fig. 6H). Together, *in vivo* and *in vitro* data identify CLCA1-TMEM16A-Cl^- current axis as an important regulator of matrix accumulation and SASP in aging. H_2S is upstream of CLCA1 as supported by abolition of increase in kidney CLCA1 expression by the administration of NaHS to aging mice (Fig. 2B, C), and, by inhibition of Cl^- current induced by CLCA1 overexpression (Fig. 6H).

Discussion

For the first time we show that CLCA1 contributes to kidney injury in aging by stimulating Cl^- current via activation of TMEM16A, a Ca^{++}-dependent Cl^- channel. Activation of Cl^- current, a cell surface phenomenon, sets off signaling events that regulate synthesis of proteins and induce SASP in proximal tubular epithelial cells (Fig. 6I). Our additional novel finding is that this system is under the regulation of H_2S.

Different types of Cl^- channels (CLC) exist in the kidney (Verkman & Galietta 2009). Eight members of CLC gene family serve as anion channels or anion-proton exchangers (Jentsch & Pusch 2018). Other types of Cl^- channels in the kidney include Cystic Fibrosis Transmembrane Conductance Regulator, Ca^{++}-dependent Cl^- channels, e.g., TMEM16A (anoctamin-1), volume-regulated anion channels, ligand gated channels, and maxi ion channels. They are involved in endosomal and lysosomal functions, and in Golgi acidification (Verkman & Galietta 2009; Jentsch & Pusch 2018). Our study involves the TMEM16A channel.

TMEM16A belongs to a family of 10 members (TMEM16A-K) (Caputo et al., 2008; Schroeder et al., 2008; Yang et al., 2013). TMEM16A is expressed in airway epithelia and smooth muscle, and is linked to mucus cell metaplasia and airway hyperactivity (Caputo et al., 2008; Huang et al., 2012; Scudieri et al., 2012). In the kidney, podocytes, proximal tubular epithelial cells, and principal epithelial cells of collecting ducts express TMEM16A (Faria et al., 2014; Schreiber et al., 2019). It is located in the apical and sub-apical membrane domains in proximal tubular epithelial cells (Faria et al., 2014). In addition to being a Cl^- channel, TMEM16A regulates albumin uptake and endosomal acidification (Faria et al., 2014). Global TMEM16A knock out mice develop albuminuria, and die postnatally due to unstable airway (Rock et al., 2008; Ousingsawat et al., 2009). Podocyte-specific TMEM16A knock out mice display normal podocyte structure and glomerular filtration associated with non-significant increase in albuminuria (Faria et al., 2014). Tubule-specific TMEM16A knock out mice develop transient proteinuria associated with retention of

endosomal vesicles in proximal tubules (Faria et al., 2014). Combined podocyte and tubular TMEM16A knock out mice have reduced glomerular number and proteinuria; proximal tubular epithelial cells show loss of cilia (Schenk et al., 2018). TMEM16A is involved in polycystic kidney disease by increasing Cl^- secretion and cyst growth (Buchholz et al., 2014; Schreiber et al., 2019). ATP, UTP, calmodulin, phosphatidylinositol 4,5-bisphosphate, ezrin, radixin, and moesin regulate TMEM16A activity (Schwiebert et al., 2002; Turner et al., 2007; Tian et al., 2011; Perez-Cornejo et al., 2012; Pritchard et al., 2014). Activation of TMEM16A is facilitated by CLCA1 which has four human and eight murine homologs; CLCA1 is secreted (Gibson et al., 2005; Yurtsever et al., 2012; Mundhenk et al., 2018). Cells in colon, small intestine, and kidney express CLCA1 (Agnel et al., 1999).

We report for the first time that kidney cortical CLCA1 expression is increased in aging as an evolutionarily conserved feature. Patch clamp studies in proximal tubular epithelial cells *in vitro* showed that overexpression of hCLCA1 resulted in increase in Cl^- current by TMEM16A activation. Increased hCLCA1 expression markedly affected signaling leading to increased matrix protein content. hCLCA1 overexpression drove Akt phosphorylation which was associated with downstream stimulation of mTORC1, and increase in matrix proteins. Similar processes of activation of Akt-mTORC1 axis also occurs in association with fibrosis in the kidney in aging mice (Lee et al., 2018). Inhibition of TMEM16A mitigated mTORC1 activation and increase in matrix proteins in hCLCA1 overexpressing cells. These data show CLCA1-TMEM16A-Cl^- axis is upstream of signaling regulation of matrix protein synthesis in the aged kidney. SASP induction by overexpression of CLCA1 may involve mTORC1 activation, a known inducer of SASP (Herranz et al., 2015). A key issue for future investigations is how the process of cell surface anion secretion should trigger SASP.

Interestingly, we found an interaction between the gasotransmitter H_2S and the CLCA1-TMEM16A-Cl^- current system. H_2S is drawing increasing attention for its ability to regulate several critical biological functions of the kidney (Kasinath et al., 2018). As mentioned in the Results section, the kidney normally generates

significant amounts of H_2S. Reduced H_2S generation occurs in several models of kidney injury including acute kidney injury due to ischemia, urinary tract obstruction, or *cis*-platinum toxicity, and, also in chronic kidney injury encountered in diabetes and hypertension including pregnancy related preeclampsia. Treatment with H_2S donors ameliorates kidney injury in these disorders (Kasinath et al., 2018). Our previous work has added kidney injury due to aging to this list. Aging kidneys have decreased expression of CSE and CBS enzymes leading to reduced H_2S generation. Administration of H_2S to aging mice ameliorates fibrosis, albuminuria, and SASP by stimulating AMPK and inhibiting mTORC1 in the kidney (Lee et al., 2018). Our studies on mechanisms underlying the salutary effect of H_2S on cell injury caused by CLCA1 overexpression also revealed that it involves stimulation of AMPK and inhibition of mTORC1. These data together demonstrate that H_2S deficiency is a proximal event in the aging kidney leading to downstream activation of CLCA1-TMEM16A- Cl^- current axis and mTORC1-regulated cell events. The latter include matrix protein synthesis and SASP (Fig. 6I) as both are linked to mTOR activation (Kasinath et al., 2009; Herranz et al., 2015). SASP has been linked to extracellular matrix remodeling and kidney fibrosis by activation of pro-fibrotic pathway including the Wnt9 and TGFβ1 pathway (Luo et al., 2018). We saw a similar recruitment of AMPK by H_2S to inhibit mTOR and matrix protein increase in high glucose treated podocytes (Lee et al., 2012). In addition, high glucose induced increase in NADPH oxidase 4 expression and subsequent oxidative injury in proximal tubule epithelial cells was also inhibited by H_2S by activating AMPK (Lee et al., 2017). These data suggest that H_2S employs a common signaling mechanism involving AMPK activation in protecting against kidney cell injury.

The mechanism by which stimulation of CLCA1-TMEM16A pathway activates Akt signaling is not clear from our studies. Increased Cl^- current may be associated with Na^+ and fluid secretion across the cell membrane altering cell shape, which can activate signaling pathways (Schmick & Bastiaens 2014). Studies are needed to address the status of Cl^- secretion in the aging kidney; data on measurement of Cl^- in excreted urine will be difficult to interpret because

of numerous other factors that regulate Cl^- transport in and out of tubular cells in the kidney. These non-CLCA1-TMEM16A determinants of Cl^- handling in the kidney include many other types of Cl^- channels, Na^+ K^+ 2Cl transporter, Cl^- anion exchangers to mention a few. Additionally, passive paracellular Cl^- transport mechanisms also exist in the kidney. Urinary Cl^- is a composite result of all these determinants.

TMEM16A promotes cyst growth in polycystic kidney disease (Schreiber et al., 2019). Aging is associated with development of kidney cysts; CLCA1-TMEM16A-Cl^- current axis could have a role in this phenomenon. Kidney cysts are common in end stage kidney disease, often associated with malignancy. These processes could also involve the CLCA1-TMEM16A-Cl^- current system.

In summary, we identify CLCA1-TMEM16A-Cl^- current axis as a novel paradigm contributing to kidney injury in aging. It could serve as an interventional target to arrest aging associated kidney injury.

Experimental Procedures

RNA-Seq for Transcriptome Profiling and Bioinformatics. RNA was extracted from the kidney cortex of C57BL6 young mice (n=4, mean age 5 months) and aged mice (n=4, mean age 32 months), using TRIzol (Cat. #, 15596018, Thermo Fisher Scientific) as previously described (Cavaglieri et al., 2015). RNA quality and integrity were checked using Agilent 2100 Bioanalyzer using RNA 6000 Nano kit (Agilent Technologies, Santa Clara, CA). Approximately 500 ng Total RNA was used for RNA-Seq library preparation by following the KAPA Stranded RNA-Seq Kit with RiboErase (HMR) sample preparation guide (Cat. #, KR1151, KAPA Biosystems). The first step in the workflow involved the depletion of rRNA by hybridization of complementary DNA oligonucleotides, followed by treatment with RNase H and DNase to remove rRNA duplexed to DNA and original DNA oligonucleotides, respectively. Following rRNA removal, the remaining RNA was fragmented into small pieces using divalent cations under elevated temperature and magnesium. The cleaved RNA fragments were copied into first strand cDNA using reverse transcriptase and random primers. This was followed by second strand cDNA synthesis using DNA polymerase I and RNase H. Strand specificity

was achieved by replacing dTTP with dUTP in the Second Strand Marking Mix (SMM). The incorporation of dUTP in the second strand synthesis effectively quenches the second strand during amplification, since the polymerase used in the assay will not incorporate past this nucleotide. These cDNA fragments then went through an end repair process, the addition of a single 'A' base, and then ligation of the adapters. The products were then purified and enriched with PCR to create the final RNA-Seq library. RNA-Seq libraries were subjected to quantification process by the combination of Qubit and Bioanalyzer, pooled for cBot amplification and subsequent sequenced with 100 bp paired-end (PE) sequencing module with Illumina HiSeq 3000 platform. After the sequencing run, demultiplexing with script bcl2fastq2 (Illumina, CA) were employed to generate the fastq file for each sample. The average of 41M PE reads was generated for each sample. All sequencing reads were aligned with their reference genome (UCSC mouse genome build mm9) using TopHat2 (Trapnell et al., 2012) with options (-r 100 --no-sort-bam --no-coverage-search --library-type fr-firststrand) and the BAM files obtained after alignment were processed using HTSeq-count (Anders et al., 2015) (with options: -s reverse -q -i gene_id) using NCBI RefSeq gene annotation for mm9 to obtain the counts per gene in all samples. Expression abundance of each gene was subsequently converted in unit of the fragment per kilobase of transcript per million transcripts mapped (FPKM). Differential expression was evaluated using DESeq (Anders & Huber 2010) to obtain fold-change, *P*-value, and adjusted *P*-value using Benjamini-Hochberg correction for multiple tests (Benjamini 1995). We selected differentially expressed genes (DEGs) based on the following criteria: 1) fold-change >1.5) adjusted *P*-value < 0.05; and 3) FPKM > 1. Gene ontology enrichment from the DEG list was performed using TopGO package (Alexa et al., 2006), and significantly enriched functions were selected based on classic Fisher's Exact test P-value < 0.05. Differential expression was visualized, such as the volcano plot, using R (https://www.r-project.org). Data are available at https://www.ncbi.nlm.nih.gov/geo/query/acc.cgi?acc=GSE155407

mRNA measurement by real time (RT)- qPCR: We employed the same RNA with RNA-Seq analysis for RT-qPCR. Total RNA was treated with DNase I for 30 min at 37°C, and then the mixture was incubated for 10 min at 80 °C to inactivate DNase I. 1 µg of RNA was used for cDNA generation using iScript RT SuperMix for RT-qPCR (Cat. #, 1708841, Bio-Rad). 2 µl of cDNAs were used for RT- qPCR using RT^2 SYBR Green ROX^{TM} RT-qPCR Mastermix (Cat. #, 330520, Qiagen) and primers for mouse *Clca1* (Cat. # PPK040451E-200, Qiagen), mouse *Tmem16A* (Cat. # PPM26917B-200, Qiagen) and mouse glyceraldehyde-3 phosphate dehydrogenase (*Gapdh*) (Cat. # PPM02946E, Qiagen). The RT-qPCR was run in a MasterCycler RealPlex4 (Eppendorf). Quantitation of the mRNAs was performed using the $2^{-\Delta\Delta Ct}$ method using *Gapdh* as a housekeeping gene (Cavaglieri et al., 2015).

Cell Culture: Murine proximal tubular epithelial (MCT) cells (kindly provided by Dr. Eric Neilson, Northwestern University, Chicago, IL) were grown in Dulbecco's modified Eagle's medium containing 7% fetal bovine serum, 5.5 mM glucose, 100 units/ml penicillin, 100 µg/ml streptomycin, and 2 mM glutamine (Mariappan et al., 2005).

Generation of human CLCA1 (hCLCA1) expressing cells: Transfection was performed employing FuGENE®HD according to the manufacturer's instructions (Promega Corporation, Madison, WI). One µg of pCMV6-hCLCA1 plasmid (Cat. #, RC218583, OriGene Technologies Inc, Rockville, MD) or pCMV-Entry plasmid (Cat. #, PS100001, OriGene Technologies Inc, Rockville, MD) were diluted in Opti-MEM (Cat. #, 31985070, Thermo Fisher Scientific). 1 x 10^5 of MCT cells were seeded onto a 12 well plate and transfected using 6 µl of FuGENE®HD transfection reagent (Cat. #, E2312, Promega Corporation) for 24 h. The cells were transferred into 6 x 96 well plates and incubated with 800 µg/ml of G418 (Cat. #, 4727878001, MiliporeSigma) for 7 days to select single clones. Single clones were expanded onto 100 mm plates for 2 weeks with 800 µg/ml of G418. hCLCA1 expression was determined in 12 vector clones and 32 hCLCA1 clones using antibodies against CLCA1 and FLAG (DDK). 5 vector clones and 6 hCLCA1 clones were chosen for experiments.

Animals: Animal experiments employing mice and marmosets were approved by the institutional Animal Care and Use Committee of the University of Texas Health, San Antonio, TX, and, the Southwest National Primate Research Center at the Texas Biomedical Research Institute, San Antonio, TX, respectively.

Aging mice: We employed 5-month old (n = 10) and 30-month old (n = 10) male C57BL6 mice (in house breeding) as young and aged, respectively. We also used kidney preparations from previously reported study in which 18- and 19 month- old male C57BL6 mice (National Institute of Aging) were randomized to receive 30 µmol/L of NaHS (Cat. #, 161527, Millipore Sigma) in drinking water (n=20) or plain water (n=14) for 5 months as previous described (Lee et al., 2018).

Aged Marmosets: We have recently reported aging associated changes in the marmoset, a non-human primate (Lee et al., 2019). To study changes in kidney CLCA1 expression in aged marmosets, we performed immunoblotting on kidney cortical lysates from 4 male young (average age 3 years), 4 female young (average age 3 years), 5 aged male (average age 16 years) and 5 aged female marmosets (average age 16 years).

Human kidneys: Kidney tissue was obtained from the unaffected parts of kidneys removed from patients undergoing surgery at the University of Michigan and processed via the tissue procurement service of the Department of Pathology. Clinical data were obtained through the honest broker office of the University of Michigan. Tissue was placed right away in RNAlater, micro-dissected into glomeruli and tubule-interstitial fractions, and isolated RNA was used for gene expression analysis using Affymetrix Human Gene 2.1 ST Array as described (Hodgin et al., 2015; Kato et al., 2016). This study was approved by the Institutional Review Board of the University of Michigan.

Immunohistochemistry: Mouse kidneys were fixed in 10% formaldehyde and embedded in paraffin, and 4-µm sections were cut. Sections were incubated with Xylene-S (Cat. # HC-700, Thermo Fisher Scientific) to remove paraffin and washed by ethanol. After deparaffinization, the slides were incubated with antigen unmasking solution (Cat. #, H3300, Vector Laboratories) at 125 ºC for 30

seconds and 90 ºC for 10 seconds using a declocking chamber (Cat. #, DC2002, Biocare Medical LLC, Pacheco, CA). The staining was performed by Vectastain ABC kit protocol (Cat. #, PK-4001, Vector Laboratories). CLCA1 antibodies were diluted (1:50) in Davinci Green diluent (Cat. #, PD-900L, Biocare Medical). After incubation with Vectastain ABC kit, the slides were incubated with ImmPACT NovaRED peroxidase substrate (Cat. #, SK-4805, Vector Laboratories) for 3-4 min at RT followed by hematoxylin staining for 2 min at RT.

Immunoblotting: Equal amount of protein lysates or renal cortical homogenates were analyzed by immunoblotting (Lee et al., 2010; Lee et al., 2015). We employed antibodies against the following; CLCA1 (Cat. #, ab180851, Abcam Plc), TMEM16A (Cat. #, ab72984, Abcam Plc), Flag (Cat. #, MA1-142, Thermo Fisher Scientific), fibronectin (Cat. #, ab2413, Abcam Plc), collagen 1α2 (Cat. #, 14695-1-AP, Proteintech Group Inc, Rosemont, IL), phospho-Ser79-acetyl-CoA carboxylase (ACC) (Cat. #, 3661, Cell Signaling Technology), ACC (Cat. #, 3662, Cell Signaling Technology), phospho-Ser473-Akt (Cat. #, 9271, Cell Signaling Technology), Akt (Cat. #, 9272, Cell Signaling Technology), phospho-Thr389-p70S6 kinase (Cat. #, 9205, Cell Signaling Technology), p70S6 kinase (Cat. #, 9202, Cell Signaling Technology), p53 (Cat. #, sc-6243, Santa Cruz Biotechnology), p21 (Cat. #, ab109199, Abcam Plc), $p16^{INK4a}$ (Cat. #, ab189034, Abcam Plc), IL-1α (Cat. #, ab7632, Abcam Plc), IL-1β (Cat. #, ab9722, Abcam Plc), IL-6 (Cat. #, ab7737, Abcam Plc), and Actin (Cat. #, A2066, Millipore Sigma).

Cl^- current measurement: Patch clamp experiments were done as previously described (Sun et al., 2015). Coverslips with cells were transferred to the recording chamber, and perfused with an external Ringer's solution of the following composition: Tetraethylammonium-Cl, 145 mM; $MgCl_2$, 1 mM; $CaCl_2$, 2 mM; Hepes, 10 mM; Glucose, 10mM; pH 7.3 was adjusted with Tris. Whole cell currents were recorded using an Axopatch 200B (Axon Instruments, Inc.). The patch pipette had resistances between 3 -5 MΩ after filling with the standard intracellular solution that contained the following: TEA-Cl, 145 mM; MgATP, 3 mM; Hepes, 10 mM; EGTA, 5 mM; pH 7.2 was adjusted with Tris. Total

$CaCl_2$ were adjusted to 300 nM. Free Ca^{2+} was calculated using WebmaxC Standard (http://www.stanford.edu/~cpatton/webmaxcS.htm). The stimulation protocol to generate current–voltage relationships consisted in 2 s-long voltage steps from − 100 to + 100 mV in 20 mV increments starting from a holding potential of − 60 mV. Currents were recorded at 2 kHz and digitized at 5–8 kHz. pClamp 10.1 software was used for data acquisition and analysis. Basal leak was subtracted from the final currents and average currents are shown. All experiments were carried out under room temperature.

Statistics: Data were expressed as mean ± SD; analyses between two groups were performed by the t test using the GraphPad Prism. Data were considered statistically significant at $p< 0.05$. Statistical comparisons between multiple subgroups were performed by ANOVA one-way, and post hoc analysis was done using Tukey multiple comparisons test, employing GraphPad Prism8.

Acknowledgements:

This work was supported by the Department of Veterans Affairs Biomedical Laboratory Research and Development Service Merit Review Award I01 BX001340 to BSK, KS. AS is supported by NIH R01 AG050797. MM is supported by NIH grant R01GM135760. MB is supported by NIH/NIDDK R01 DK100449. GGC is supported by VA merit Review Award 2I01 BX000926 and Research Career Scientist Award IK6BX00361. BBS is supported by R01DE017102 from the NIH. KS is supported by the VA Merit Review Award 1I01BX003234. Sequencing data was generated in the Genome Sequencing Facility which is supported by UTHSA, NIH-NCI P30 CA054174 (Cancer Center at UT Health San Antonio) to YC and CPRIT Core Facility Award RP160732 to YC, and NIH-NCATS 1UL1 TR002645-01 (NIH CTSA) to YC. This work was also supported by the Pathology Core of the San Antonio Nathan Shock Center (P30-AG013319) -YI. The San Antonio Marmoset Aging Program is supported by NIH P51 OD011133, and P30 AG044271 (CR). This work is partially supported by George O'Brien Michigan Kidney Translational Core Center at University of Michigan, funded by NIH/NIDDK grant 2P30-DK-081943. We thank Dr. James Nelson for critical reading of the manuscript.

Conflict of Interest Statement

Kumar Sharma is on the Data Safety Monitoring Board of Sanofi and Cara Therapeutics. All other authors declare that they have no conflict of interest.

Author contributions:

BSK supervised the project in its conception, design, data interpretation, and wrote the manuscript. HJL contributed to the design and conducted experiments with the aid of AD. YS and BBS designed and conducted patch clamp experiments. AS, YI, CR, YD, CLO, WJ, MB helped in collecting and interpreting data on kidney samples from experimental animals and humans. YC supervised RNA Seq data collection and interpretation. DF, GGC, MM, BBS, YC, and KS participated in data interpretation, and writing of the manuscript. All authors provided input, and approved the manuscript.

Data and Materials Availability Statement

RNA Seq data are available at:
https://www.ncbi.nlm.nih.gov/geo/query/acc.cgi?acc=GSE155407
Cultured proximal tubule cells stably transfected with hCLCA1 are available on request.

References

Agnel, M., Vermat, T. , Culouscou, J. M. (1999). Identification of three novel members of the calcium-dependent chloride channel (CaCC) family predominantly expressed in the digestive tract and trachea. *FEBS Lett*. **455**, 295-301. 10.1016/s0014-5793(99)00891-1

Alexa, A., Rahnenfuhrer, J. , Lengauer, T. (2006). Improved scoring of functional groups from gene expression data by decorrelating GO graph structure. *Bioinformatics*. **22**, 1600-1607. 10.1093/bioinformatics/btl140

Anders, S. , Huber, W. (2010). Differential expression analysis for sequence count data. *Genome Biol*. **11**, R106. 10.1186/gb-2010-11-10-r106

Anders, S., Pyl, P. T. , Huber, W. (2015). HTSeq--a Python framework to work with high-throughput sequencing data. *Bioinformatics*. **31**, 166-169. 10.1093/bioinformatics/btu638

Baker, D. J., Childs, B. G., Durik, M., Wijers, M. E., Sieben, C. J., Zhong, J., . . . van Deursen, J. M. (2016). Naturally occurring p16(Ink4a)-positive cells shorten healthy lifespan. *Nature*. **530**, 184-189. 10.1038/nature16932

Benjamini, Y. a. H., Y. (1995). Controlling the false discovery rate: A practical and powerful approach to multiple testing. . *J Royal Stat Soc*. **57**, 289-300.

Bitzer, M. , Wiggins, J. (2016). Aging Biology in the Kidney. *Adv Chronic Kidney Dis*. **23**, 12-18. 10.1053/j.ackd.2015.11.005

Buchholz, B., Schley, G., Faria, D., Kroening, S., Willam, C., Schreiber, R., . . . Eckardt, K. U. (2014). Hypoxia-inducible factor-1alpha causes renal cyst expansion through calcium-activated chloride secretion. *J Am Soc Nephrol*. **25**, 465-474. 10.1681/ASN.2013030209

Caputo, A., Caci, E., Ferrera, L., Pedemonte, N., Barsanti, C., Sondo, E., . . . Galietta, L. J. (2008). TMEM16A, a membrane protein associated with calcium-dependent chloride channel activity. *Science*. **322**, 590-594. 10.1126/science.1163518

Cavaglieri, R. C., Day, R. T., Feliers, D. , Abboud, H. E. (2015). Metformin prevents renal interstitial fibrosis in mice with unilateral ureteral obstruction. *Mol Cell Endocrinol*. **412**, 116-122. 10.1016/j.mce.2015.06.006

Faria, D., Rock, J. R., Romao, A. M., Schweda, F., Bandulik, S., Witzgall, R., . . . Schreiber, R. (2014). The calcium-activated chloride channel Anoctamin 1 contributes to the regulation of renal function. *Kidney Int*. **85**, 1369-1381. 10.1038/ki.2013.535

Feliers, D., Lee, H. J. , Kasinath, B. S. (2016). Hydrogen Sulfide in Renal Physiology and Disease. *Antioxidants & redox signaling*. **25**, 720-731. 10.1089/ars.2015.6596

Gibson, A., Lewis, A. P., Affleck, K., Aitken, A. J., Meldrum, E. , Thompson, N. (2005). hCLCA1 and mCLCA3 are secreted non-integral membrane proteins and therefore are not ion channels. *J Biol Chem*. **280**, 27205-27212. 10.1074/jbc.M504654200

Hawley, S. A., Ross, F. A., Gowans, G. J., Tibarewal, P., Leslie, N. R. , Hardie, D. G. (2014). Phosphorylation by Akt within the ST loop of AMPK-alpha1 down-regulates its activation in tumour cells. *Biochem J*. **459**, 275-287. 10.1042/BJ20131344

Herranz, N., Gallage, S., Mellone, M., Wuestefeld, T., Klotz, S., Hanley, C. J., . . . Gil, J. (2015). mTOR regulates MAPKAPK2 translation to control the senescence-associated secretory phenotype. *Nat Cell Biol*. **17**, 1205-1217. 10.1038/ncb3225

Hodgin, J. B., Bitzer, M., Wickman, L., Afshinnia, F., Wang, S. Q., O'Connor, C., . . . Wiggins, R. C. (2015). Glomerular Aging and Focal Global Glomerulosclerosis: A Podometric Perspective. *Journal of the American Society of Nephrology : JASN*. **26**, 3162-3178. 10.1681/ASN.2014080752

Huang, F., Zhang, H., Wu, M., Yang, H., Kudo, M., Peters, C. J., . . . Rock, J. R. (2012). Calcium-activated chloride channel TMEM16A modulates mucin secretion and airway smooth muscle contraction. *Proc Natl Acad Sci U S A*. **109**, 16354-16359. 10.1073/pnas.1214596109

Humphreys, B. D. (2018). Mechanisms of Renal Fibrosis. *Annu Rev Physiol*. **80**, 309-326. 10.1146/annurev-physiol-022516-034227

Jentsch, T. J. , Pusch, M. (2018). CLC Chloride Channels and Transporters: Structure, Function, Physiology, and Disease. *Physiol Rev*. **98**, 1493-1590. 10.1152/physrev.00047.2017

Kasinath, B. S., Feliers, D. , Lee, H. J. (2018). Hydrogen sulfide as a regulatory factor in kidney health and disease. *Biochem Pharmacol*. **149**, 29-41. 10.1016/j.bcp.2017.12.005

Kasinath, B. S., Feliers, D., Sataranatarajan, K., Ghosh Choudhury, G., Lee, M. J. , Mariappan, M. M. (2009). Regulation of mRNA translation in renal physiology and disease. *Am J Physiol Renal Physiol*. **297**, F1153-1165. 10.1152/ajprenal.90748.2008

Kato, M., Wang, M., Chen, Z., Bhatt, K., Oh, H. J., Lanting, L., . . . Natarajan, R. (2016). An endoplasmic reticulum stress-regulated lncRNA hosting a

microRNA megacluster induces early features of diabetic nephropathy. *Nature communications*. **7**, 12864. 10.1038/ncomms12864

Lee, H. J., Feliers, D., Barnes, J. L., Oh, S., Choudhury, G. G., Diaz, V., . . . Kasinath, B. S. (2018). Hydrogen sulfide ameliorates aging-associated changes in the kidney. *Geroscience*. **40**, 163-176. 10.1007/s11357-018-0018-y

Lee, H. J., Feliers, D., Mariappan, M. M., Sataranatarajan, K., Choudhury, G. G., Gorin, Y. , Kasinath, B. S. (2015). Tadalafil Integrates Nitric Oxide-Hydrogen Sulfide Signaling to Inhibit High Glucose-induced Matrix Protein Synthesis in Podocytes. *J Biol Chem*. **290**, 12014-12026. 10.1074/jbc.M114.615377

Lee, H. J., Gonzalez, O., Dick, E. J., Donati, A., Feliers, D., Choudhury, G. G., . . . Kasinath, B. S. (2019). Marmoset as a Model to Study Kidney Changes Associated With Aging. *J Gerontol A Biol Sci Med Sci*. **74**, 315-324. 10.1093/gerona/gly237

Lee, H. J., Lee, D. Y., Mariappan, M. M., Feliers, D., Ghosh-Choudhury, G., Abboud, H. E., . . . Kasinath, B. S. (2017). Hydrogen sulfide inhibits high glucose-induced NADPH oxidase 4 expression and matrix increase by recruiting inducible nitric oxide synthase in kidney proximal tubular epithelial cells. *The Journal of biological chemistry*. **292**, 5665-5675. 10.1074/jbc.M116.766758

Lee, H. J., Mariappan, M. M., Feliers, D., Cavaglieri, R. C., Sataranatarajan, K., Abboud, H. E., . . . Kasinath, B. S. (2012). Hydrogen sulfide inhibits high glucose-induced matrix protein synthesis by activating AMP-activated protein kinase in renal epithelial cells. *J Biol Chem*. **287**, 4451-4461. 10.1074/jbc.M111.278325

Lee, M. J., Feliers, D., Mariappan, M. M., Sataranatarajan, K., Mahimainathan, L., Musi, N., . . . Kasinath, B. S. (2007). A role for AMP-activated protein kinase in diabetes-induced renal hypertrophy. *Am J Physiol Renal Physiol*. **292**, F617-627. 10.1152/ajprenal.00278.2006

Lee, M. J., Feliers, D., Sataranatarajan, K., Mariappan, M. M., Li, M., Barnes, J. L., . . . Kasinath, B. S. (2010). Resveratrol ameliorates high glucose-induced protein synthesis in glomerular epithelial cells. *Cell Signal*. **22**, 65-70. 10.1016/j.cellsig.2009.09.011

Luo, C., Zhou, S., Zhou, Z., Liu, Y., Yang, L., Liu, J., . . . Zhou, L. (2018). Wnt9a Promotes Renal Fibrosis by Accelerating Cellular Senescence in Tubular Epithelial Cells. *J Am Soc Nephrol*. **29**, 1238-1256. 10.1681/ASN.2017050574

Mariappan, M. M., Senthil, D., Natarajan, K. S., Choudhury, G. G. , Kasinath, B. S. (2005). Phospholipase Cgamma-Erk Axis in vascular endothelial growth factor-induced eukaryotic initiation factor 4E phosphorylation and protein synthesis in renal epithelial cells. *J Biol Chem*. **280**, 28402-28411. 10.1074/jbc.M504861200

Mundhenk, L., Erickson, N. A., Klymiuk, N. , Gruber, A. D. (2018). Interspecies diversity of chloride channel regulators, calcium-activated 3 genes. *PLoS One*. **13**, e0191512. 10.1371/journal.pone.0191512

Ousingsawat, J., Martins, J. R., Schreiber, R., Rock, J. R., Harfe, B. D. , Kunzelmann, K. (2009). Loss of TMEM16A causes a defect in epithelial Ca2+-dependent chloride transport. *J Biol Chem*. **284**, 28698-28703. 10.1074/jbc.M109.012120

Perez-Cornejo, P., Gokhale, A., Duran, C., Cui, Y., Xiao, Q., Hartzell, H. C. , Faundez, V. (2012). Anoctamin 1 (Tmem16A) Ca2+-activated chloride channel stoichiometrically interacts with an ezrin-radixin-moesin network. *Proc Natl Acad Sci U S A*. **109**, 10376-10381. 10.1073/pnas.1200174109

Pritchard, H. A., Leblanc, N., Albert, A. P. , Greenwood, I. A. (2014). Inhibitory role of phosphatidylinositol 4,5-bisphosphate on TMEM16A-encoded calcium-activated chloride channels in rat pulmonary artery. *Br J Pharmacol*. **171**, 4311-4321. 10.1111/bph.12778

Rock, J. R., Futtner, C. R. , Harfe, B. D. (2008). The transmembrane protein TMEM16A is required for normal development of the murine trachea. *Dev Biol*. **321**, 141-149. 10.1016/j.ydbio.2008.06.009

Sala-Rabanal, M., Yurtsever, Z., Berry, K. N., Nichols, C. G. , Brett, T. J. (2017). Modulation of TMEM16A channel activity by the von Willebrand factor type A (VWA) domain of the calcium-activated chloride channel regulator 1 (CLCA1). *J Biol Chem*. **292**, 9164-9174. 10.1074/jbc.M117.788232

Sala-Rabanal, M., Yurtsever, Z., Nichols, C. G. , Brett, T. J. (2015). Secreted CLCA1 modulates TMEM16A to activate Ca(2+)-dependent chloride currents in human cells. *Elife*. **4**. 10.7554/eLife.05875

Sarbassov, D. D., Guertin, D. A., Ali, S. M. , Sabatini, D. M. (2005). Phosphorylation and regulation of Akt/PKB by the rictor-mTOR complex. *Science*. **307**, 1098-1101. 10.1126/science.1106148

Sataranatarajan, K., Feliers, D., Mariappan, M. M., Lee, H. J., Lee, M. J., Day, R. T., . . . Kasinath, B. S. (2012). Molecular events in matrix protein metabolism in the aging kidney. *Aging Cell*. **11**, 1065-1073. 10.1111/acel.12008

Sataranatarajan, K., Mariappan, M. M., Lee, M. J., Feliers, D., Choudhury, G. G., Barnes, J. L. , Kasinath, B. S. (2007). Regulation of elongation phase of mRNA translation in diabetic nephropathy: amelioration by rapamycin. *Am J Pathol*. **171**, 1733-1742. 10.2353/ajpath.2007.070412

Schenk, L. K., Buchholz, B., Henke, S. F., Michgehl, U., Daniel, C., Amann, K., . . . Pavenstadt, H. (2018). Nephron-specific knockout of TMEM16A leads to reduced number of glomeruli and albuminuria. *Am J Physiol Renal Physiol*. **315**, F1777-F1786. 10.1152/ajprenal.00638.2017

Schmick, M. , Bastiaens, P. I. H. (2014). The interdependence of membrane shape and cellular signal processing. *Cell*. **156**, 1132-1138. 10.1016/j.cell.2014.02.007

Schreiber, R., Buchholz, B., Kraus, A., Schley, G., Scholz, J., Ousingsawat, J. , Kunzelmann, K. (2019). Lipid Peroxidation Drives Renal Cyst Growth In Vitro through Activation of TMEM16A. *J Am Soc Nephrol*. **30**, 228-242. 10.1681/ASN.2018010039

Schroeder, B. C., Cheng, T., Jan, Y. N. , Jan, L. Y. (2008). Expression cloning of TMEM16A as a calcium-activated chloride channel subunit. *Cell*. **134**, 1019-1029. 10.1016/j.cell.2008.09.003

Schwiebert, E. M., Wallace, D. P., Braunstein, G. M., King, S. R., Peti-Peterdi, J., Hanaoka, K., . . . Taylor, A. L. (2002). Autocrine extracellular purinergic signaling in epithelial cells derived from polycystic kidneys. *Am J Physiol Renal Physiol*. **282**, F763-775. 10.1152/ajprenal.0337.2000

Scudieri, P., Caci, E., Bruno, S., Ferrera, L., Schiavon, M., Sondo, E., . . . Galietta, L. J. (2012). Association of TMEM16A chloride channel overexpression with airway goblet cell metaplasia. *J Physiol*. **590**, 6141-6155. 10.1113/jphysiol.2012.240838

Sun, Y., Birnbaumer, L. , Singh, B. B. (2015). TRPC1 regulates calcium-activated chloride channels in salivary gland cells. *J Cell Physiol*. **230**, 2848-2856. 10.1002/jcp.25017

Tian, Y., Kongsuphol, P., Hug, M., Ousingsawat, J., Witzgall, R., Schreiber, R. , Kunzelmann, K. (2011). Calmodulin-dependent activation of the epithelial calcium-dependent chloride channel TMEM16A. *FASEB J*. **25**, 1058-1068. 10.1096/fj.10-166884

Trapnell, C., Roberts, A., Goff, L., Pertea, G., Kim, D., Kelley, D. R., . . . Pachter, L. (2012). Differential gene and transcript expression analysis of RNA-seq experiments with TopHat and Cufflinks. *Nat Protoc*. **7**, 562-578. 10.1038/nprot.2012.016

Turner, C. M., King, B. F., Srai, K. S. , Unwin, R. J. (2007). Antagonism of endogenous putative P2Y receptors reduces the growth of MDCK-derived cysts cultured in vitro. *Am J Physiol Renal Physiol*. **292**, F15-25. 10.1152/ajprenal.00103.2006

Verkman, A. S. , Galietta, L. J. (2009). Chloride channels as drug targets. *Nat Rev Drug Discov*. **8**, 153-171. 10.1038/nrd2780

Wu, J., Zhang, R., Torreggiani, M., Ting, A., Xiong, H., Striker, G. E., . . . Zheng, F. (2010). Induction of diabetes in aged C57B6 mice results in severe nephropathy: an association with oxidative stress, endoplasmic reticulum

stress, and inflammation. *Am J Pathol*. **176**, 2163-2176. 10.2353/ajpath.2010.090386

Xu, J., Zhou, L. , Liu, Y. (2020). Cellular Senescence in Kidney Fibrosis: Pathologic Significance and Therapeutic Strategies. *Front Pharmacol*. **11**, 601325. 10.3389/fphar.2020.601325

Yang, B., Cao, L., Liu, B., McCaig, C. D. , Pu, J. (2013). The transition from proliferation to differentiation in colorectal cancer is regulated by the calcium activated chloride channel A1. *PLoS One*. **8**, e60861. 10.1371/journal.pone.0060861

Yurtsever, Z., Sala-Rabanal, M., Randolph, D. T., Scheaffer, S. M., Roswit, W. T., Alevy, Y. G., . . . Brett, T. J. (2012). Self-cleavage of human CLCA1 protein by a novel internal metalloprotease domain controls calcium-activated chloride channel activation. *J Biol Chem*. **287**, 42138-42149. 10.1074/jbc.M112.410282

Zheng, F., Plati, A. R., Potier, M., Schulman, Y., Berho, M., Banerjee, A., . . . Striker, G. E. (2003). Resistance to glomerulosclerosis in B6 mice disappears after menopause. *Am J Pathol*. **162**, 1339-1348. 10.1016/S0002-9440(10)63929-6

Zhou, X., Feng, Y., Zhan, Z. , Chen, J. (2014). Hydrogen sulfide alleviates diabetic nephropathy in a streptozotocin-induced diabetic rat model. *The Journal of biological chemistry*. **289**, 28827-28834. 10.1074/jbc.M114.596593

Supplemental Material Table of Contents

Supplementary Figures

S1. Aging is associated with increased kidney CLCA1 expression in marmosets. Immunoblotting of kidney cortex of young and aged female marmosets showed increased expression of the 72 kDa fragment of CLCA1, probably the N-terminal fragment. A trend towards increase in the expression of the whole 130 kDa molecule was seen in the same animals.

S2. Rapamycin abolished the increase in phosphorylation of p70S6 kinase in hCLCA1 overexpressing cells indicating inhibition of mTORC1.

Supplementary Table

Table 1. List of mRNAs that were differentially regulated in renal cortex of aged mice.

Table 2. Top hits on RNA Seq and their possible functions.

Figure legends

Figure 1. Aging is associated with increase in the kidney CLCA1 expression in mice and humans. A. HEAT map shows distribution of kidney mRNAs that were significantly increased (red) or decreased (green) in the aged mice (n=4) vs. young mice (n=4)**.** The location of *Clca1* is shown. **B.** A volcano plot of mRNA changes in renal cortex of young mice and aged mice. *Clca1* expression was increased in the kidneys of aged mice (arrow). **C.** RT-qPCR using specific primers showed increase in renal cortical *Clca1* mRNA in aged mice (n=4) vs. young mice (n=4). **D.** Immunoblotting showed increase in CLCA1 protein expression in the renal cortex of aged mice (n=10) compared to young mice (n=10). **E.** Immunoblotting did not show change in the expression of TMEM16A in kidneys of aged mice (n=10) vs. young mice (n=10). **F.** GO analysis of cellular component of regulated kidney mRNAs showed that extracellular region part and extracellular space were among the major hits. **G.** GO analysis for molecular function revealed anion transmembrane activity and secondary active transmembrane transporter activity among the top hits. **H.** GO analysis for biologic process identified small molecule metabolic process as one of the top findings. C, D, E. Data (mean ± SD) are shown in bars with scatter plots, and were analyzed by t-test. *p<0.05, **p<0.01.

Figure 2. Histologic analysis of kidney CLCA1 expression. A. On immunoperoxidase staining (x200) a faint tubular expression of CLCA1 was seen in kidney cortex from young mice, which was robustly increased in aged mice. Representative images from young (n=4 mice) and aged mice are shown (n=4).

B, C. Administration of NaHS to 18-19-month old aging mice daily for 5 months (n=20) (Aging NaHS) reduced renal cortical CLCLA1 expression by immunoblotting compared to aging mice receiving water vehicle (Aging Con) (n=14) (B). This was confirmed by immunoperoxidase staining (x200) (C). **D.** There was a direct correlation between age and *CLCA1* expression in the tubule interstitium compartment in the kidney tissue from human subjects (n=24). B. Data (mean ± SD) are shown in bars with scatter plots and were analyzed by t-test. ***p<0.001.

Figure 3. Overexpression of hCLCA1 increases matrix protein and induces changes in signaling kinases in proximal tubular epithelial cells *in vitro*. A. Immunoblotting showed increased CLCA1 expression (130 kDa) and probably of its N-terminal fragment (72 kDa) in cells stably transfected with hCLCA1 (6 clones) vs. control plasmid transfected clones (5 clones); bands from 3 control and 4 hCLCA1 overexpressing clones are shown. **B.** hCLCA1 overexpression did not alter TMEM16A expression. **C.** Whole cell patch clamp showed increase in Cl^- current in hCLCA1 overexpressing cells vs. vector-transfected controls (mock). Cl^- current was abolished by T16Ainh-A01 in both mock and hCLCA1 overexpressing cells. **D.** Overexpression of hCLCA1 resulted in increase in matrix protein fibronectin. **E-F.** Immunoblotting with specific antibodies showed decrease in ACC phosphorylation, and increase in p70S6 kinase phosphorylation. **G.** Incubation with 25 nM rapamycin for 30 min abolished the increase in fibronectin expression seen following overexpression of hCLCA1 (data from 3 experiments are shown). **H.** Overexpression of hCLCA1 increased Akt phosphorylation at Ser473. Data (mean ± SD) are shown in bars in scatter plots and were analyzed by t-test (B, D-F, and H) or ANOVA (G). *p<0.05, **p<0.01, ***p<0.001. D, E, F, H employed 5 control and 6 hCLCA1 clones.

Figure 4. SASP is induced by overexpression of hCLCA1 in proximal tubular epithelial cells *in vitro*. A-C. Overexpression of hCLCA1 resulted in increase in the expression of p53, p21 and $p16^{INK4a}$. **D-F.** Increased expression of IL-1α, IL-1β and IL-6 was seen in cells overexpressing hCLCA1. Data (mean ±

SD) are shown in bars with scatter plots and were analyzed by t-test. *p<0.05, **p<0.01, ***p<0.001. (A-F, 5 control and 6 hCLCA1 clones were employed).

Figure 5. TMEM16A inhibition abolishes changes in fibronectin and SASP induced by overexpression of hCLCA1 in proximal tubular epithelial cells in vitro. A-C. T16Ainh-A01, a selective TMEM16A inhibitor, inhibited increase in matrix fibronectin induced by hCLCA1 overexpression vs. vector-transfected controls without affecting the expression of CLCA1 and TMEM16A. **D-H.** T16Ainh-A01 abolished hCLCA1-overexpression-induced increase in p53, p21, $p16^{INK4a}$, IL-1β and IL-6. Data from 3-4 experiments (mean ± SD) are shown in scatter plots and were analyzed by ANOVA. *p<0.05, **p<0.01, ***p<0.001.

Figure 6. Interaction between overexpression of hCLCA1 and H_2S in proximal tubular epithelial cells *in vitro*. A. Expression of CSE but not CBS, enzymes in the trans-sulfuration pathway involved in H_2S generation, was decreased by overexpression of hCLCA1. **B.** Increased hCLCA1 expression did not affect H_2S generation in MCT cells. **C.** NaHS abolished the increase in fibronectin expression induced by overexpression of hCLCA1. **D.** AMPK activity as assessed by phosphorylation of its substrate ACC was inhibited by overexpression of hCLCA1, which was abolished by NaHS. **E.** Activity of mTORC1 as evaluated by phosphorylation of its substrate p70S6 kinase was increased by hCLCA1 overexpression, which was reduced by NaHS. **F, G.** NaHS inhibited some aspects of SASP, i.e., increase in $p16^{INK4a}$ and IL-1β, induced by overexpression of hCLCA1. Data from 4 experiments (mean ± SD) are shown in bars with scatter plots and were analyzed by ANOVA. *p<0.05, **p<0.01, ***p<0.001. **H.** Patch clamp studies: addition of NaHS inhibited Cl^- current induced by hCLCA-1 overexpression. **I.** A schematic summarizes the role of CLCA1-TMEM16A-Cl^- current in aging-associated kidney injury.

Figure 1

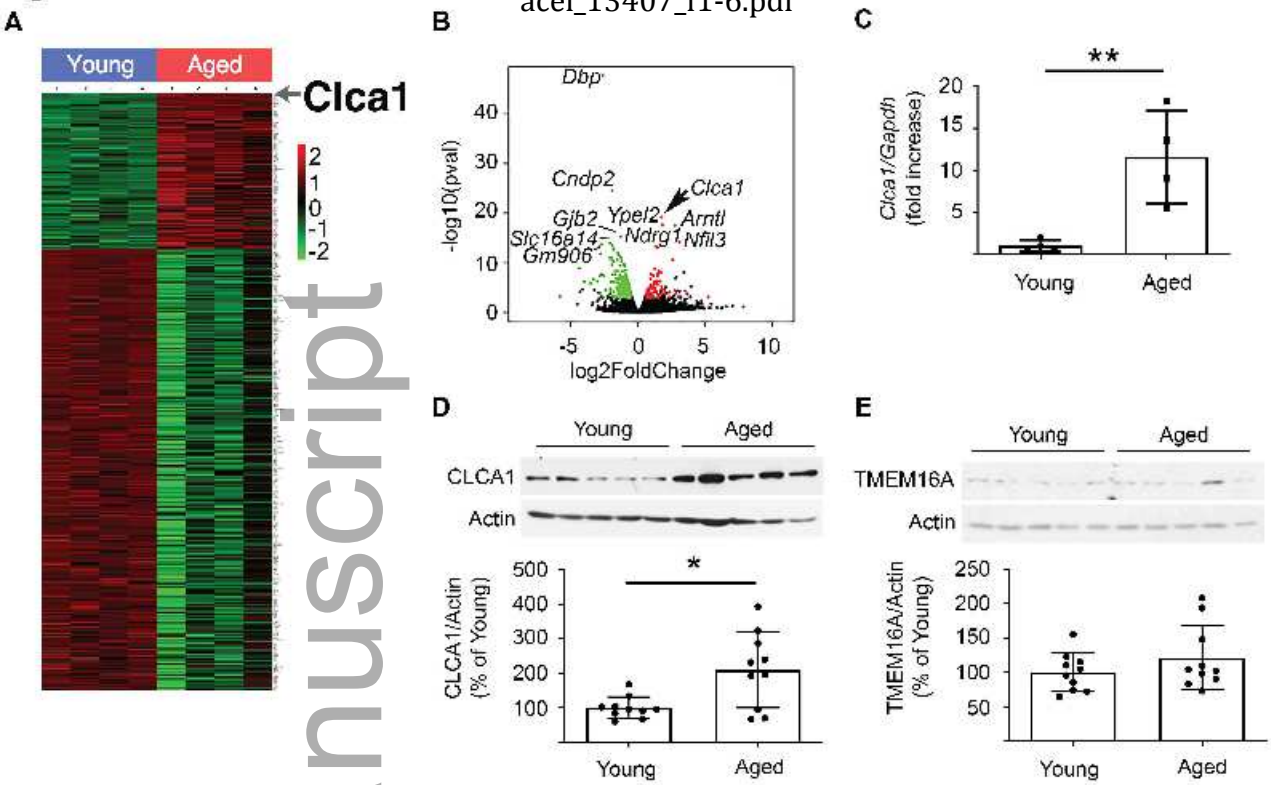

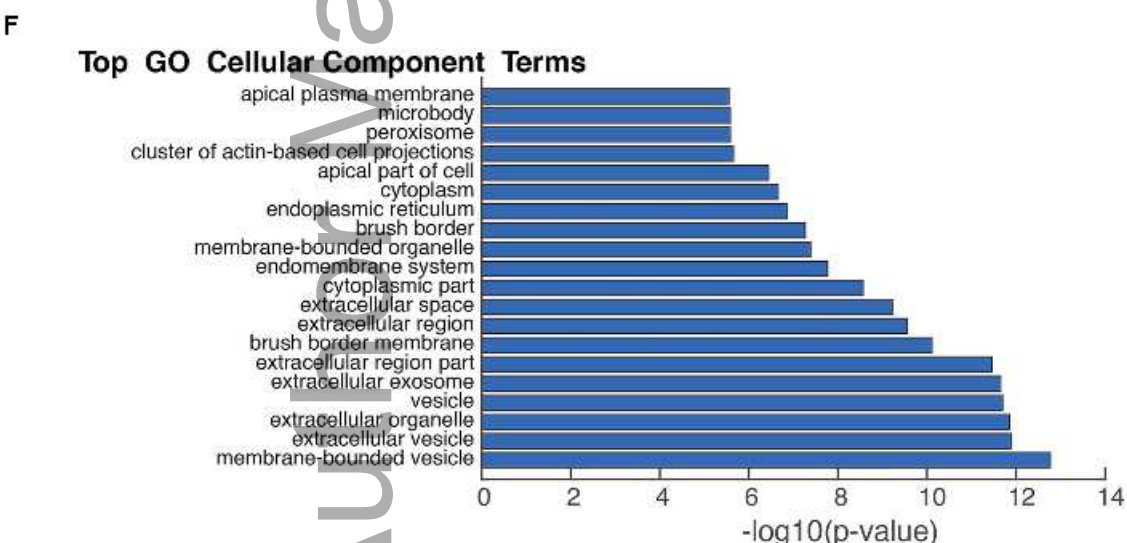

G

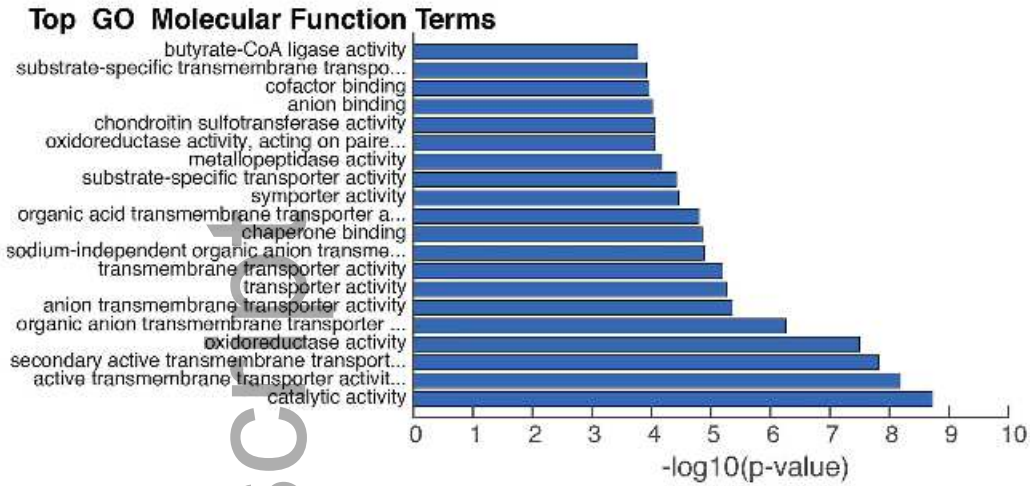

H

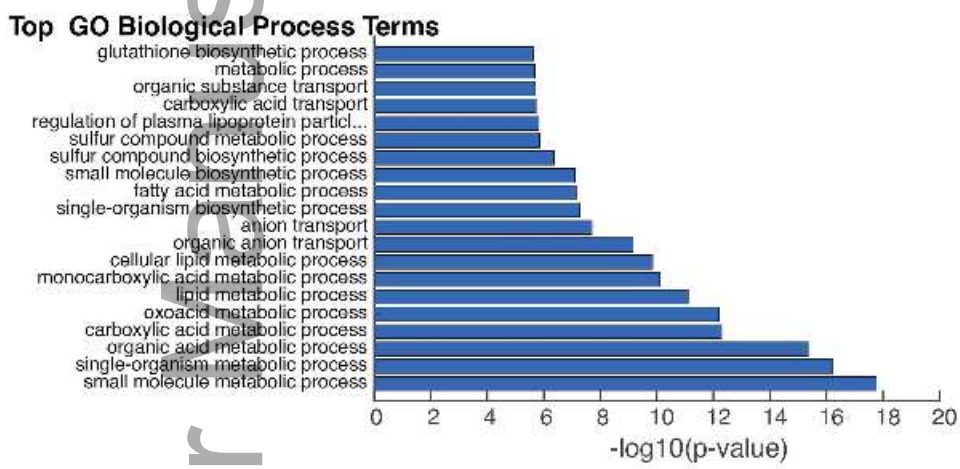

Figure 2

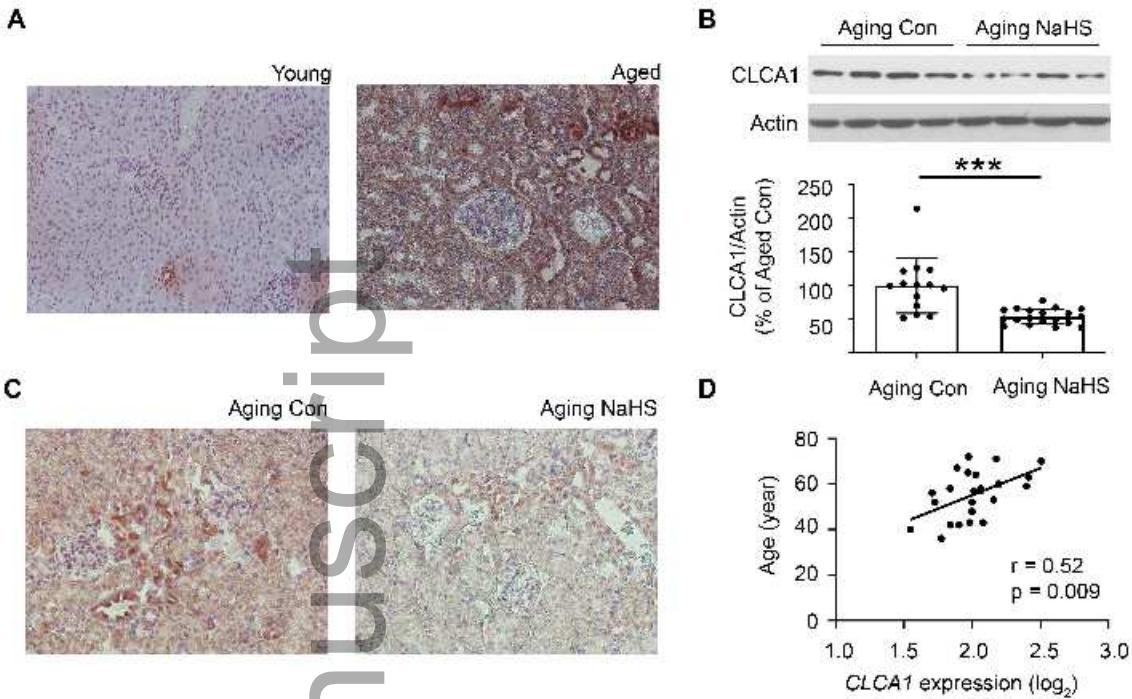

Figure 3

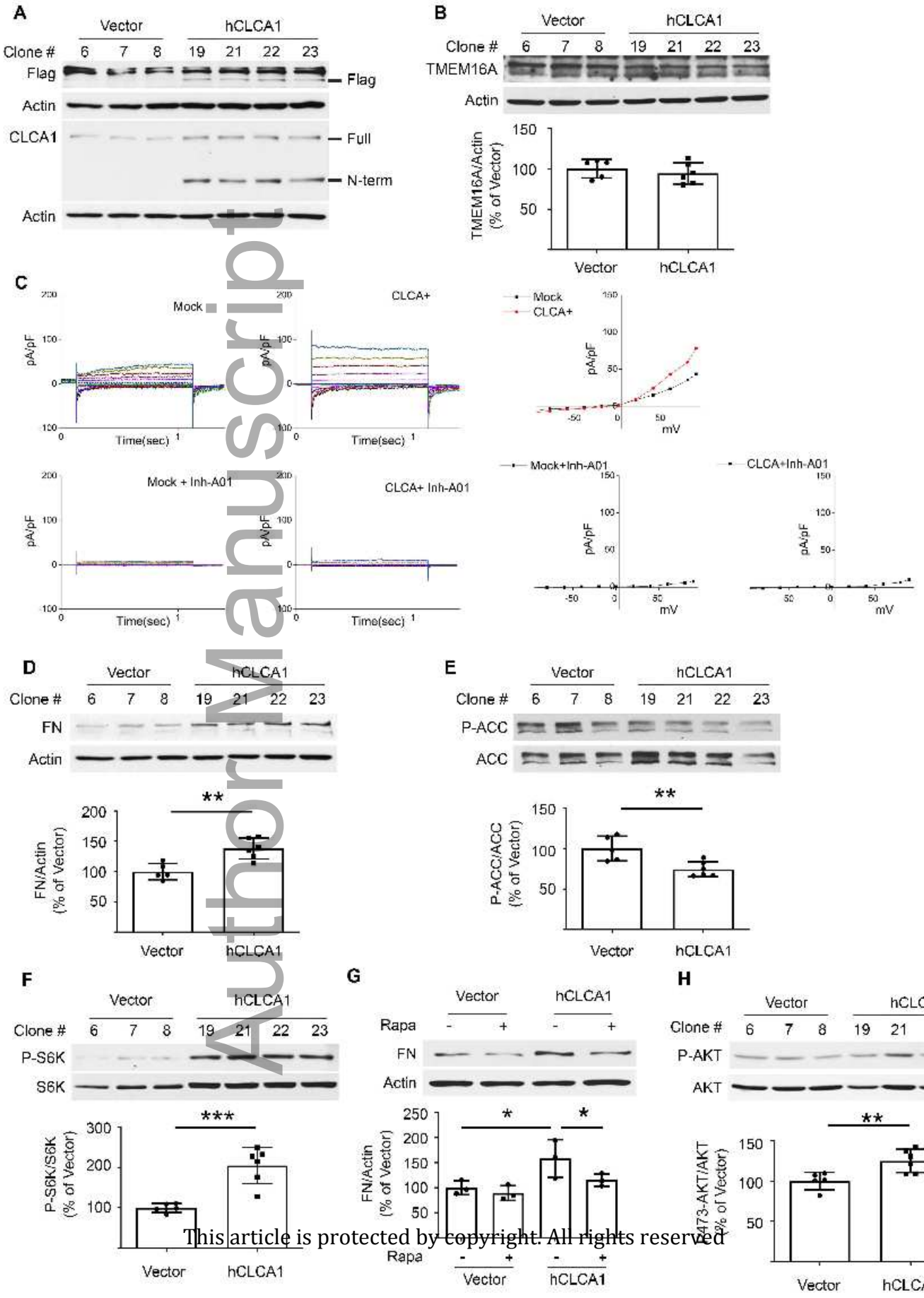

Figure 4

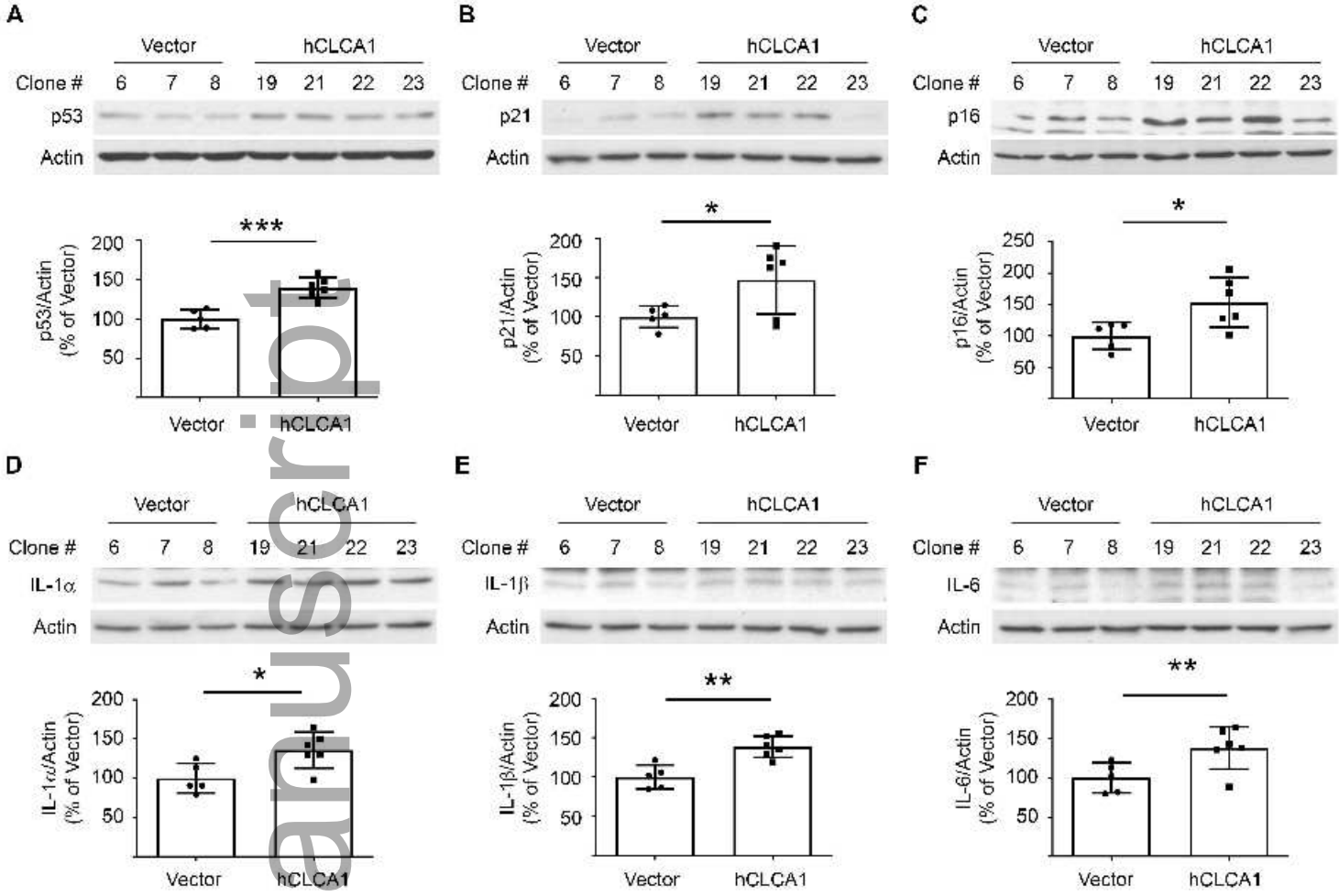

Figure 5

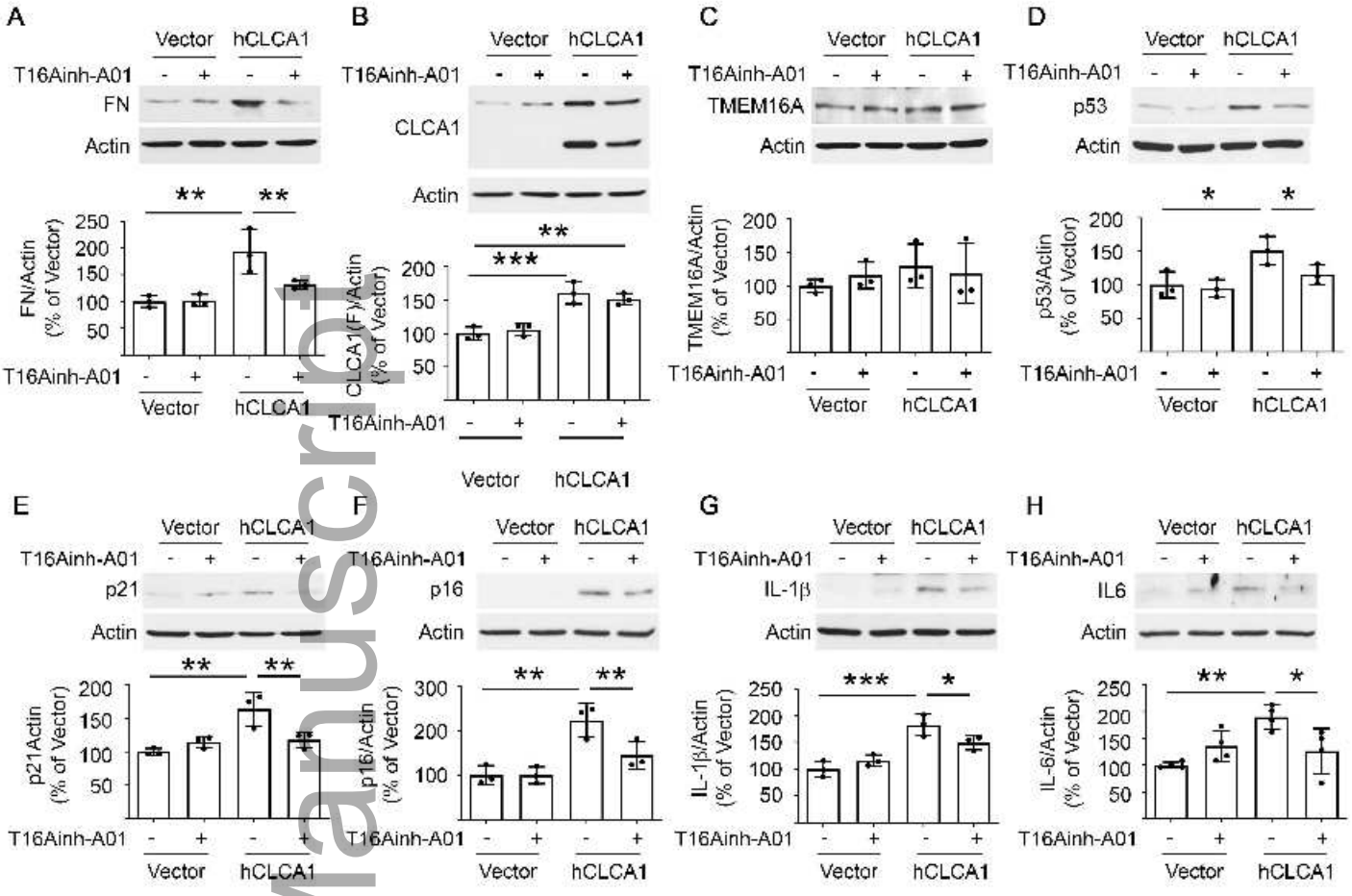

Figure 6